Digest Journal of Nanomaterials and Biostructures Vol. 13, No. 3, July - September 2018, p. 595 - 601

Ln^{3+} DOPED UPCONVERSION NANOPARTICLES FOR POTENTIAL DUAL MODAL BIO-IMAGING APPLICATION

X. J. LI*, K. J. WU, W. Q. ZHANG, Z. G. QI
College of Materials Science and Engineering, Harbin University of Science and Technology, Harbin, China

Bimodal bioimaging probes have raised wide concern in recent years for remedying shortcomings inherent to one given imaging technology. Rare-earth upconversion nanoparticles (UCNPs) which can absorb low-energy photons and emit high energy photons have attracted great interest not only because of their unique application in upconversion luminescence imaging, but also because they can generate visible emission by near-infrared radiation (NIR) excitation. Here we have synthesized PEI capped Ln^{3+} doped $NaGdF_4$ UCNPs in a one-pot facile hydrothermal method in order to meet the demand for upconversion luminescence (UCL) and magnetic resonance imaging (MRI) simultaneously. PEI used here endows these NPs with good water solubility and biocompatibility. The properties of the nanoparticles were confirmed by transmission electron microscopy, X-ray powder diffraction, Fourier transform-infrared, and upconversion luminescence spectra and magnetism. Further biocompatibility test has also been investigated. The results indicate that our synthesized nanoparticles have potential application in bio-imaging probes combining UCL and MRI modal imaging together.

(Received February 7, 2018; Accepted July 2, 2017)

Keywords: Upconversion, Nanoparticle, Bio-probe

1. Introduction

Multimodal bioimaging has sparked considerable interest in biology and medicine, which contains kinds of imaging modality, such as optical, ultrasound, nuclear, X-ray computed tomography (CT) and magnetic resonance imaging (MRI) [1-3]. In addition to therapeutic applications which require bi- or multimodal vectors, there is also much excitement about the possibility of combining two or more imaging techniques, in order to remedy shortcomings inherent for one given imaging technology [4]. For example, MRI is a noninvasive diagnostic tool and could provide unsurpassed three-dimensional soft tissue detail and various lesions information about brain, spine and chest and no ionizing radiation to normal tissue cells, but has relatively low sensitivity [5-7]. When combining near-infrared optical imaging with MRI, the problem of sensitivity and resolution that arises from one single imaging technique could be solved [8,9]. Thus multimodal bio-imaging could satisfy the higher requirements on the efficiency and accuracy for clinical diagnosis and medical research [10-12].

Compared with conventional materials, nano-materials benefiting from the significantly improved physical, chemical and biological properties have been widely used for bioimaging and simultaneous diagnosis and therapy [13,14]. As we all know, lanthanide ions with longer metastable level lifetime enabling sequential photon absorption are particularly suitable for producing high efficiency upconversion process because of superior photostability, low toxicity, non-blinking emission and narrow emission peak [15,16]. When intergrating with nanotechnology, lanthanide ions-doped nanoparticles have shown fascinate foreground in biology/biomedicine, especially in multimodal bioimaging. For example, lanthanide doped nanoparticles (NPs) can be used for the generation of visible emission by NIR excitation of which is significant in exploiting NIR probes [17]. As a significant lanthanide ion, Gd^{3+} has seven unpaired inner 4f electrons that are effectively

*Corresponding author: lixuejiao@hrbust.edu.cn

shielded by the outer electrons $5s^2 5p^6$ from the external microenvironment, at the same time Gd^{3+} ion has large magnetic moment and long electronic relaxation time which has been used as contrast agents for MR imaging [18]. Moreover, resulting from the lowest excited level ($^6F_{7/2}$) of Gd^{3+} far higher than most excited level of Yb^{3+} and Er^{3+}, the excitation energy loss through energy transfer from Yb^{3+} and Er^{3+} to Gd^{3+} involved in the UC processes can be avoided [19,20]. Thus by co-doping Gd^{3+}, Yb^{3+} and Er^{3+} RE ions in nanoparticles, a multifunctional nanoparticles possessing the advantages of fluorescent and magnetic properties could be achievable and have potential applications as NIR/MRI probe [21,22].

In our work, we have synthesized multifunctional PEI capped $NaGdF_4$: Yb^{3+}, Er^{3+} nanoparticals (NPs) as biological probes in a one-pot facile hydrothermal method [23]. Compared with previous methods, hydrothermal method is relatively safe and environmentally friendly. Here PEI, a dendrigraft cationic polymer was coated on the surface of obtained NPs during the hydrothermal process, which played double roles in forming multifunctional NPs. On the one hand, it endows these NPs with good water solubility and biocompatibility. Moreover, the free amine groups on the surface of the NPs provide functional groups to bond with specific ligand molecules. On the other hand, high cationic charge density makes PEI as a gene delivery vector both in vitro and in vivo early since 1995 [24,25]. In conclusion, our prepared magnetic and luminescent NPs can not only provide substantially enhanced UCL and MR signals signals with nanometer resolution in monitoring of physiological processes, but also may have potential to create a platform for subsequent gene therapy in living cells, tissues and organisms [26-28].

2. Experimental section

2.1 Chemicals and materials

Polyethylenimine (PEI, branched polymer $(-NHCH_2CH_2-)_x$ $(-N(CH_2CH_2NH_2)CH_2CH_2-)_y$) were purchased from Aldrich. The rare earth oxides RE_2O_3 (99.99%) (RE = Gd, Yb, Er,) were purchased from Science and Technology Parent Company of Changchun Institute of Applied Chemistry and other chemicals were purchased from Beijing Chemical Co., Ltd. $Gd(NO_3)_3$, $Er(NO_3)_3$ and $Yb(NO_3)_3$ crystals were prepared by dissolving corresponding rare earth oxides in dilute HNO_3 and heating, then dissolved in ethylene glycol (0.5 M). All chemicals are of analytical grade reagents and used directly without further purification.

2.2 Synthesis of Water Dispersible PEI capped UCNPs

In a typical procedure for preparing $NaGdF_4$ particles, 0.2g PEI, 1.2 mmol of NaCl and 1.2 mL $RECl_3$ (0.5M, RE: 80%Gd^{3+}, 17%Yb^{3+}, 3%Er^{3+} mole ratio) were first added into 7.8 mL of ethylene glycol under vigorous stirring until forming a transparent solution. Subsequently, 3.6 mmol NH_4F was added into 9 mL ethylene glycol. After vigorous stirring for 15 min, the two solutions above were mixed together, and then transferred into a 50 mL Teflon autoclave, which was tightly sealed and maintained at 200 °C for only 45 min. As the autoclave was cooled to the room temperature naturally, the NPs obtained were collected by centrifugation, washed three times with ethanol and deionized water, and finally dispersed in 5mL H_2O.

2.3 The biocompatibility of the prepared PEI-UCNPs

To evaluate the biocompatibility of the PEI-UCNPs, MTT cell assay was performed on the L929 cell. MTT is a standard test for screening the toxicity of biomaterials and is carried out in accordance with ASTM standards. Briefly, L929 fibroblast cells were plated out at a density of 5000-6000 cells per well in a 96 well plate, leave 8 wells empty for blank controls, then incubated overnight at 37°C in a humidified atmosphere of 5% CO_2 to allow the cells to attach to the wells. The PEI-UCNPs were sterilized by autoclaving, and then serial dilutions of the nanocomposites at concentrations of 3.125, 6.25, 12.5, 25, 50, 100, and 200 μg/mL were added to the culture wells to replace the original culture medium and incubated for another 24 h in 5% CO_2 at 37 °C. 5 mg/mL stock solution of MTT [3-(4,5-dimethylthiazol-2-yl)-2,5-diphenyltetrazolium bromide] was prepared in PBS and this stock solution (20 μL, 0.8 mg/mL) was added to each well containing a different amount of the monodisperse PEI-UCNPs for another 4 h. Then 150 μL of dimethyl sulfoxide (DMSO) was added to each well before the plate was examined using a microplate reader (Therom Multiskan MK3) at the wavelength of 490 nm.

2.4 Characterization

The X-ray diffraction (XRD) pattern of the sample was carried out on a D8 Focus diffractometer (Bruker) with use of Cu Kα radiation (λ = 0.15405 nm). Transmission electron microscopy (TEM) micrographs were recorded from a FEI Tecnai G2 S-Twin transmission electron microscope with a field emission gun operating at 200 kV. Fourier-transform Infrared spectra were measured on a Vertex Perkin-Elmer 580BIR spectrophotometer (Bruker) with the KBr pellet technique. The UC emission spectra were determined on an F-7000 spectrophotometer (Hitachi) equipped using a 980 nm laser as the excitation source. The T_1-weighted MR images were obtained using a 0.55T MRI magnet (Shanghai Niumag Corporation Ration NM120-Analyst).

3. Results and discussion

3.1 Phase and Morphology of the UCNPs

The synthesis of Ln^{3+}-doped $NaGdF_4$ UCNPs as ideal bio-probes was developed by means of an efficient and environmentally friendly hydrothermal procedure with PEI as gene vector, surfactant and capping agent. Fig. 1 shows the wide-angle XRD patterns of the standard card (JCPDS No. 27-0699).

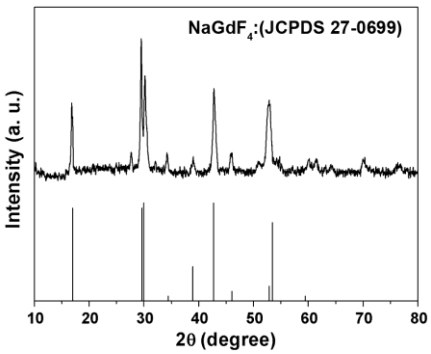

Fig. 1. XRD patterns of $NaGdF_4$ UCNPs.

The results of the XRD indicate that the as-synthesized $NaGdF_4$:Yb^{3+}, Er^{3+} samples are well crystallized, and the patterns are consistent with hexagonal phase structure of $NaGdF_4$.

As depicted in Fig. 2, the as-prepared PEI capped UCNPs in Figure 2b are uniform and the average diameter is about 60 nm according to the TEM image.

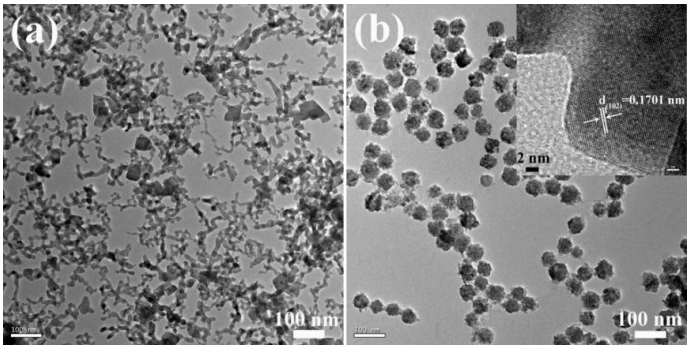

Fig. 2. TEM of synthesized $NaGdF_4$:Yb^{3+}/Er^{3+} (17/3 mol%) nanoparticles without PEI (a) and PEI capped nanoparticles (b). Inset is the HRTEM image.

In contrast, the NPs without adding PEI when prepared were also shown in Fig. 2a. Here as a surfactant, PEI was added to control particle size and morphology, as well as modulate the dispersion of these particles [29]. The high-resolution TEM (HRTEM) image of UCNPs confirms the high crystallinity of the particles with a d-spacing value of 0.1701 nm, which is close to the d_{102} value of hexagonal-phase $NaGdF_4$ (inset of Fig. 2b).

3.2 Structural Analysis of the UCNPs

To demonstrate the existence of PEI on the nanoparticles, the FT-IR spectra of the PEI-UCNPs (Fig. 3b) was compared with that of pure UCNPs synthesized without PEI (Fig. 3a).

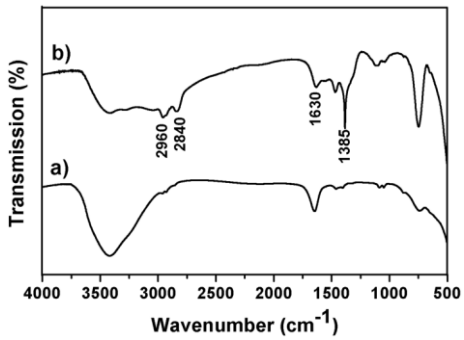

Fig. 3. FT-IR spectra of prepared UCNPs without PEI (a) synthetic PEI capped UCNPs (b).

The presence of PEI is confirmed by the presence of the unique absorption peaks from internal vibration of the amide bonds (1385–1630 cm^{-1}) and CH_2 stretching vibrations (2840–2960 cm^{-1}) in the spectrum from PEI-UCNPs only [30]. The presence of free amine groups on the surface of the nanoparticles is of extreme importance since these can bond with the ligand molecule necessary for additional functionalization of the nanoparticle.

3.2 Upconvertion and magnetism property of the UCNPs

Lanthanide-doped upconversion NPs usually offer high photostability and enable deep tissue-penetration depths (up to 10 mm) by irradiation with near-infrared (NIR) light, which makes them particularly attractive for bioimaging applications. As the initial energy transfer, an electron of the Yb^{3+} ion is excited from the $^2F_{7/2}$ to $^2F_{5/2}$ level by the NIR light due to its strong absorption at 980 nm, and then an excited Yb^{3+} transfer its energy to Er^{3+} ($^4I_{11/2}$). During the lifetime of the $^4I_{11/2}$ level, a second 980 nm photon transferred by the excited Yb^{3+} ion can then populate a higher $^4F_{7/2}$ energetic state of the Er^{3+} ion, whose energy lies in the visible region.

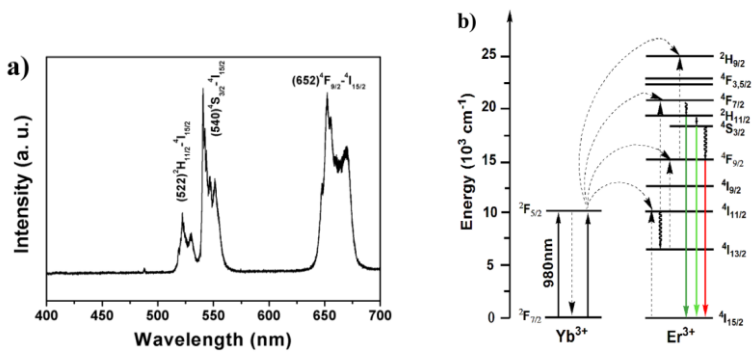

Fig. 4. The emission spectra of the UCNPs (a); Schematic energy-level diagrams of the Yb^{3+}, Er^{3+} ions and the UC mechanism excited by 980 nm laser diode (b).

As shown in Fig. 4, the Er^{3+} ion can then relax nonradiatively by a fast multi-phonon relaxation process to the $^2H_{11/2}$ and $^4S_{3/2}$ levels and radiant transitions from these levels yield emissions at 522 nm ($^2H_{11/2}\rightarrow{}^4I_{15/2}$), 540 nm ($^4S_{3/2}\rightarrow{}^4I_{15/2}$). Alternatively, the electron can further relax and populate the $^4F_{9/2}$ level resulting in the occurrence of red $^4F_{9/2}\rightarrow{}^4I_{15/2}$ (652 nm) emission [31-33].

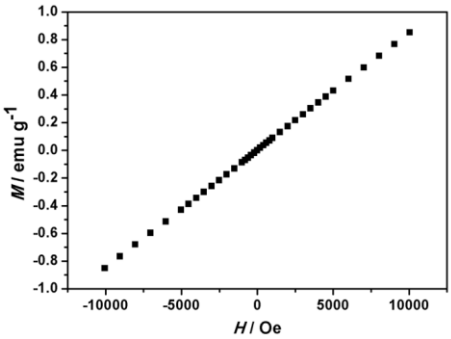

Fig. 5. Magnetization curves of Ln^{3+}-doped $NaGdF_4$ UCNCs.

Apart from the aforementioned luminescence properties, the $NaGdF_4$ UCNPs show typical paramagnetism at room temperature (Fig. 5). The mass magnetic susceptibility of UCNPs was determined to be $(8.507\pm0.001)\times10^{-5}$ $emuOe^{-1}g^{-1}$ from the magnetization slope, which can be used for magnetic resonance imaging.

3.3 In vitro cytotoxicity of the UCNPs

For potential applications in bio-probes, it is critically important to evaluate the toxicity of PEI-UCNPs. As far as we know, the lanthanides based UC luminescent materials have been reported to exhibit no or low cytotoxicity in vivo in some literatures. Although free PEI has been reported to be toxic to cells, when it is in particulate form, the detrimental effects are greatly lessened (Park et al. 2012). Here MTT assays were performed on L929 cell lines to evaluate the cytotoxicity of our samples. As shown in Fig. 6, PEI-UCNPs showed no significant cytotoxic effect on the L929 cells at 3.125-200 μg/mL after incubation for 24 h. The cell viability can even reach 96.49% with the concentration as high as 200 μg/mL. The results above demonstrate that our samples have good biocompatibility and have potential to be used in biological imaging.

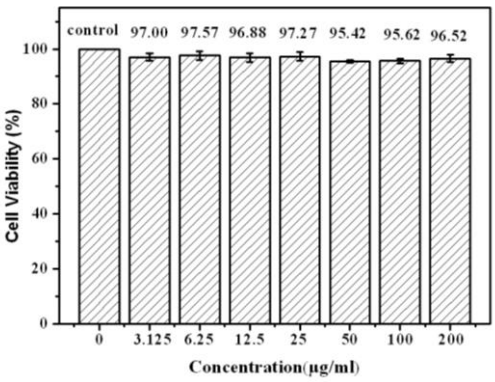

Fig. 6. The L929 fibroblast cells viability after incubating with UCNPs for 24 h and quantitative assays by standard MTT method.

4. Conclusions

In summary, we have synthesized monodisperse water-soluble hexagonal Ln^{3+}-doped $NaGdF_4$: Yb^{3+}, Er^{3+} UCNPs by means of a fast, facile and environmentally friendly hydrothermal process by using PEI as surfactant. The prepared $NaGdF_4$ nanoparticles show the attracting

properties of good water solubility, biocompatibility, excellent stability and UC emission and paramagnetism which are suitable for biologic application. The multi-functional imaging system could bring novel opportunities to the next generation of probes for the detection and imaging.

Acknowledgements

This project is financially supported by Natural Science Foundation of Heilongjiang Province (No.QC2017056) and National college students innovation and entrepreneurship training program (201610214023).

References

[1] N. Bogdan, E. M. Rodriguez, F. Sanz-Rodriguez, M. C. Iglesias de la Cruz, A. Juarranz, D. Jaque, J. G. Sole, J. A. Capobianco, Nanoscale **4**(12), 3647 (2012).
[2] G. Wang, Q. Peng, Y. Li, Accounts of Chemical Research **44**(5), 322 (2011).
[3] J. Kim, Y. Piao, T. Hyeon, Chemical Society Reviews **38**(2), 372 (2009).
[4] C. W. Park, Y. S. Rhee, F. G. Vogt, D. Hayes, J. B. Zwischenberger, P. P. DeLuca, H. M. Mansour, Adv. Drug. Deliv. Rev. **64**(4), 344 (2012).
[5] F. Barkhof, J. H. Simon, F. Fazekas, M. Rovaris, L. Kappos, N. de Stefano, C. H. Polman, J. Petkau, E. W. Radue, M. P. Sormani, D. K. Li, P. O'Connor, X. Montalban, D. H. Miller, M. Filippi Nat. Rev. Neurol. **8**(1), 13 (2012).
[6] N. J. J. Johnson, W. Oakden, G. J. Stanisz, R. S. Prosser, F. C. J. M. van Veggel Size-Tunable, Chemistry of Materials **23**(21), 4877(2011).
[7] X. Zhu, J. Zhou, M. Chen, M. Shi, W. Feng, F. Li, Biomaterials **33**(18), 4618(2012).
[8] C. S. Bonnet, F. Buron, F. Caille, C. M. Shade, B. Drahos, L. Pellegatti, J. Zhang, S. Villette, L. Helm, C. Pichon, F. Suzenet, S. Petoud, E. Toth, Chem.-Eur. J. **18**(5), 1419 (2012).
[9] P. Sharma, N. E. Bengtsson, G. A. Walter, H. B. Sohn, G. Y. Zhou, N. Iwakuma, H. D. Zeng, S. R. Grobmyer, E. W. Scott, B. M. Moudgil, Small **8**(18), 2856 (2012) 2868
[10] F. Caille, C. S. Bonnet, F. Buron, S. Villette, L. Helm, S. Petoud, F. Suzenet, E. Toth, Inorg. Chem. **51**(4), 2522 (2012).
[11] X. Y. Wang, S. H. Ju, C. Li, X. G. Peng, A. F. Chen, H. Mao, G. J. Teng, PLoS One 7 (11) (2012).
[12] H. Y. Xing, W. B. Bu, S. J. Zhang, X. P. Zheng, M. Li, F. Chen, Q. J. He, L. P. Zhou, W. J. Peng, Y. Q. Hua, J. L. Shi, Biomaterials **33**(4), 1079 (2012).
[13] S. Huang, C. Li, Z. Cheng, Y. Fan, P. Yang, C. Zhang, K. Yang, J. Lin, J. Colloid. Interface. Sci. **376**, 312 (2012).
[14] Y. Liu, D. Tu, H. Zhu, X. Chen, Chem. Soc. Rev. **42**(16), 6924 (2013).
[15] F. Wang, D. Banerjee, Y. S. Liu, X. Y. Chen, X. G. Liu, Analyst. **135**(8), 1839 (2010).
[16] L. Y. Wang, R. X. Yan, Z. Y. Hao, L. Wang, J. H. Zeng, H. Bao, X. Wang, Q. Peng, Y. D. Li, Angew. Chem.-Int. Edit. **44**(37), 6054(2005).
[17] C. Wang, H. Q. Tao, L. Cheng, Z. Liu, Biomaterials **32**(26), 6145 (2011b).
[18] Y. L. Liu, K. L. Ai, Q. H. Yuan, L. H. Lu, Biomaterials **32**(4), 1185 (2011).
[19] Y. A. Wu, C. X. Li, D. M. Yang, J. Lin, J. Colloid. Interface. Sci. **354**(2), 429 (2011).
[20] F. Zhang, D. Y. Zhao, ACS Nano **3**(1), 159 (2009).
[21] Q. Ju, D. Tu, Y. Liu, R. Li, H. Zhu, J. Chen, Z. Chen, M. Huang, X. Chen, Journal of the American Chemical Society **134**(2), 1323 (2011).
[22] F. Li, C. Li, X. Liu, Y. Chen, T. Bai, L. Wang, Z. Shi, S. Feng, Hydrophilic, Chemistry – A European Journal **18**(37), 11641 (2012).
[23] Q. Ju, D. T. Tu, Y. S. Liu, R. F. Li, H. M. Zhu, J. C. Chen, Z. Chen, M. D. Huang, X. Y. Chen Journal of the American Chemical Society **134**(2), 1323 (2012).
[24] O. Boussif, F. Lezoualc'h, M. A. Zanta, M. D. Mergny, D. Scherman, B. Demeneix, J. P. Behr, Proceedings of the National Academy of Sciences **92**(16), 7297 (1995).
[25] S. Patnaik, K. C. Gupta, Expert Opin. Drug. Deliv. **10**(2), 215 (2013).
[26] H. Kobayashi, P. L. Choyke, Accounts of Chemical Research **44**(2), 83 (2011).
[27] F. B. A. Yu, P. Li, G. Y. Li, G. J. Zhao, T. S. Chu, K. L. Han, Journal of the American Chemical Society **133**(29), 11030 (2011).

[28] F. M. Kievit, O. Veiseh, N. Bhattarai, C. Fang, J. W. Gunn, D. Lee, R. G. Ellenbogen, J. M. Olson, M. Zhang, Advanced Functional Materials **19**(14), 2244 (2009).
[29] F. Wang, D. K. Chatterjee, Z. Li, Y. Zhang, X. Fan, M. Wang, Nanotechnology **17**(23), 5786 (2006).
[30] H. Petersen, P. M. Fechner, A. L. Martin, K. Kunath, S. Stolnik, C. J. Roberts, D. Fischer, M. C. Davies, T. Kissel, Bioconjugate Chem. **13**(4), 845 (2002).
[31] M. Haase, H. Schäfer, Angewandte Chemie International Edition **50**(26), 5808 (2011).
[32] Y. P. Li, J. H. Zhang, X. Zhang, Y. S. Luo, X. G. Ren, H. F. Zhao, X. J. Wang, L. D. Sun, C. H. Yan, J. Phys. Chem. C **113**(11), 4413(2009).
[33] Q. Liu, T. Yang, W. Feng, F. Li, Journal of the American Chemical Society 1**3**4(11), 5390 (2012).